Composites: Part B 50 (2013) 273–278

Contents lists available at SciVerse ScienceDirect

Composites: Part B

journal homepage: www.elsevier.com/locate/compositesb

Miscibility studies of some semi-interpenetrating polymer networks based on an aromatic polyurethane and epoxy resin

Cristian-Dragos Varganici [a], Liliana Rosu [a], Dan Rosu [a,*], Bogdan C. Simionescu [a,b]

[a] Centre of Advanced Research in Bionanoconjugates and Biopolymers, "Petru Poni" Institute of Macromolecular Chemistry, 41A Gigore Ghica-Voda Alley, 700487 Iasi, Romania
[b] Department of Natural and Synthetic Polymers, "Gh. Asachi" Technical University of Iasi, 73 Dimitrie Mangeron Boulevard, 700050 Iasi, Romania

ARTICLE INFO

Article history:
Received 26 November 2012
Received in revised form 31 January 2013
Accepted 6 February 2013
Available online 22 February 2013

Keywords:
A. Polymer–matrix composites (PMCs)
B. High-temperature properties
B. Interface/interphase
B. Microstructures

ABSTRACT

Glass transition temperatures of some semi-interpenetrating polymer networks based on aromatic polyurethane and cross-linked epoxy resin were determined by differential scanning calorimetry. The influence of increasing epoxy network content on the glass transition temperatures was studied. Absolute heat capacities and cross-linking densities were determined. It was observed that the glass transition temperatures increased with increasing epoxy resin content until phase separation. Miscibility studies were conducted by applying Fox and Gordon–Taylor equations. Morphological studies were conducted by optical microscopy and scanning electron microscopy.

1. Introduction

Epoxies are reactive thermosetting resins which have the advantages of presenting multiple cross-linking possibilities and their networks exhibit superior physical properties such as good adhesion to metals and high mechanical strength [1–3]. However, there exist a series of limitations in the future applications of the pure epoxy resins such as easy stress cracking under impact forces, brittleness and stress after curing [4–6]. In order to surpass these impediments and improve their physico-chemical properties, a proposed way consists in mixing them with elastomers. Blending processes between two or more polymers may improve some physical properties of the final mixture relative to the individual pure comprising polymers characteristics [7]. However, the lack of miscibility between the comprising polymers often limits the blending process [8]. Therefore, semi-interpenetrating networks must be synthesized. Such networks are particular blends comprised of chemically dissimilar cross-linked polymer chains not chemically linked between them [8,9]. When a polymer with linear structure is entangled at molecular scale in the network of another polymer with cross-linked structure a semi-interpenetrating polymer network (S-IPN) is formed. S-IPN structures obtained between thermosetting resins such as epoxy resins or modified epoxy resins and elastomeric materials such as polyurethanes are known in literature [8–12]. Epoxies and polyurethanes provide the best overall combinations of film properties than any other organic coatings and are applied for protection of masonry and/or concrete constructions because the linear polyurethanes have excellent elasticity, abrasive resistance and damping properties and the epoxy resins networks present the above mentioned advantages.

In this paper authors report the results of miscibility studies of some S-IPN samples based on linear polyurethane and increasing epoxy resin network (ERN) content. The structures were characterized by differential scanning calorimetry (DSC), optical microscopy (OM) and scanning electron microscopy (SEM).

2. Experimental

2.1. Materials

The numeric average molecular weight (Mn) of the polyurethane elastomer (PU), measured by gel permeation chromatography, was 120.000. The molar ratio of the components poly(ethylene adipate)diol (PEA), butylene glycol (BG) and 4,40-diphenylmethane diisocyanate (MDI) was 1:5:6.

The epoxy resin (ER) was a commercial product obtained from 4,4′ isopropylidenediphenol and epichlorohydrin (Policolor Bucharest, Romania) as Ropoxid 501. The ER has the Mn value equal to 380 and an epoxy equivalent of 0.525 equiv/100 g. Ethylenediamine, purchased from Aldrich, was used as curing agent for the epoxy resin.

* Corresponding author. Tel.: +40 232 217454; fax: +40 232 211299.
E-mail addresses: drosu@icmpp.ro, dan_rosu50@yahoo.com (D. Rosu).

1359-8368/$ - see front matter © 2013 Elsevier Ltd. All rights reserved.
http://dx.doi.org/10.1016/j.compositesb.2013.02.005

2.2. Synthesis of S-IPNs

S-IPNs with increasing ERN content of 5% (S-IPN-1), 10% (S-IPN-2), 15% (S-IPN-3), 20% (S-IPN-4), 30% (S-IPN-5) and 40% (S-IPN-6) were synthesized (Scheme 1) and their synthesis was reported in a previous paper [13]. According to the reported procedure, the solution of polymers was cast as films on glass sides and was kept for 24 h at room temperature. The resulting films were washed with water in order to remove solvent traces. Afterwards the films were detached from the glass support and were maintained for 10 h at 80 °C in order to remove the traces of amine.

2.3. Characterization

2.3.1. Differential scanning calorimetry

DSC curves were recorded on a DSC 200 F3 Maia device (Netzsch, Germany). A mass of 10 mg of each sample was heated in pressed and pierced aluminum crucibles at a heating rate of 10 °C min^{-1}. Nitrogen was used as inert atmosphere at a flow rate of 50 mL min^{-1}. The temperature against heat flow was recorded. The baseline was obtained by scanning the temperature domain of the experiments with an empty pan. The enthalpy was calibrated with an indium standard as well as the heat capacity was calibrated by measuring with sapphire disk supplied by Netzsch. The temperature calibration was performed by using indium as standard metal at various heating rates.

2.3.2. Optical micrographs

Optical images of the films were obtained by means of Leica DM2500M microscope, using a 5× objective with numerical aperture of 0.12.

2.3.3. Scanning electron microscopy

Morphological studies of the S-IPN films were performed using a scanning electron microscope (Quanta 200-FEI). Environmental scanning electron microscopy (ESEM) was used in order to determine the morphology, size and elemental composition of the samples. The Quanta 200 scanning electron microscope equipped with an EDX system allows quantitative and qualitative compositional analysis.

Double-sided carbon tape was used to mount the samples on aluminum stubs. SEM investigations were performed in Low Vacuum mode using a secondary electron detector ETD at accelerating voltage of 20 kV.

3. Results and discussion

3.1. Glass transition measurements

Fig. 1 presents the heating curves (Fig. 1a) and cooling curves (Fig. 1b) of the pure polyurethane (PU) and of the S-IPN networks. The DSC heating curve of the ERN, recorded up to 600 °C, in the same experimental conditions, was reported in a previous paper. Due to its cross-linked structure the ERN showed no melting profile and only a glass transition (T_g) at 120 °C [14]. It is a fact that the synthesis of such networks determines a forced compatibilization upon the pure polymeric components [15]. A good miscibility between the comprising polymers is indicated by the presence of a single glass transition temperature (T_g) [16,17]. The composition and T_g values of the initial polymers and of the network structures are listed in Table 1.

As it can be observed from Fig. 1 and Table 1, the studied S-IPNs show a single composition-dependent T_g. The T_g values slowly shifts to upper temperature ranges with ERN percentage increase. This aspect is due to the reduction of free volume between chain segments, thus weakening their motion by sterical hindering [18,19]. The melting/crystallization profile of the pure PU decreases in intensity with cross-linking density increase up to sample S-IPN-5. This is also a sign of compatibility of the comprising polymers in the S-IPN structures. In a previous paper, no significant differences were observed between the melting peak intensities of S-IPNs with low epoxy resin content (5%, 10%). An important decrease in the intensity of the melting peaks was presented by the other samples with higher epoxy resin content (15%, 20%). The melting process DSC signals completely disappeared for samples with higher than 20% epoxy resin content. This general behavior of the melting pattern was explained by the increase of the cross-linking density of high content epoxy resin in S-IPN samples. This aspect was further confirmed by the decreasing in melting heat values [14]. Sample S-IPN-5 presents the highest T_g value of the network, indicating that 30% ERN content yields a max-

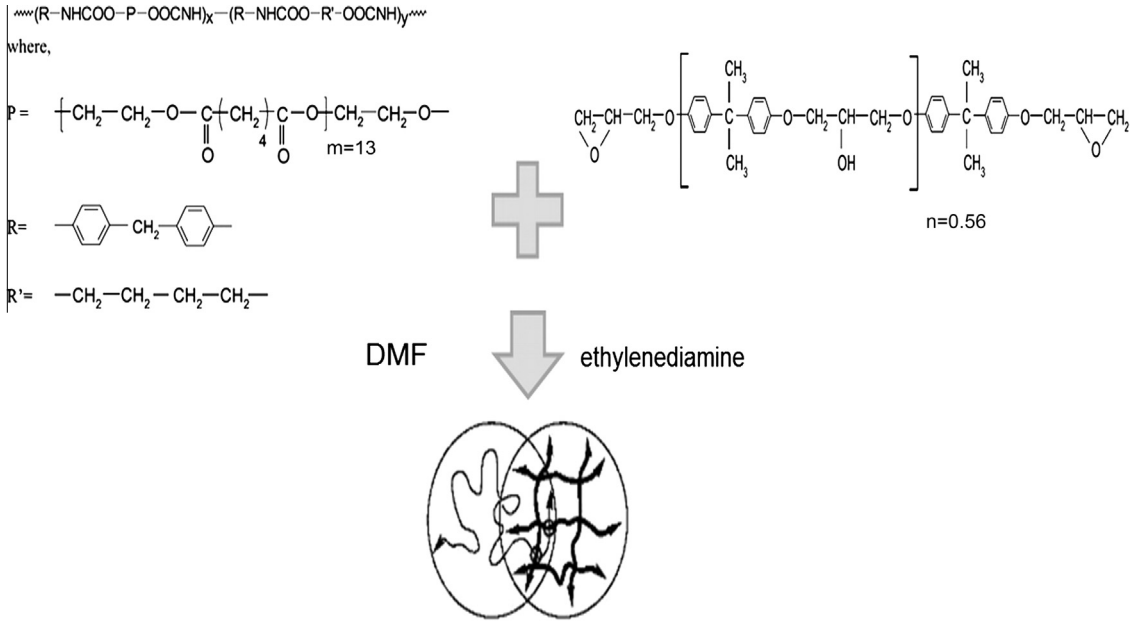

Scheme 1.

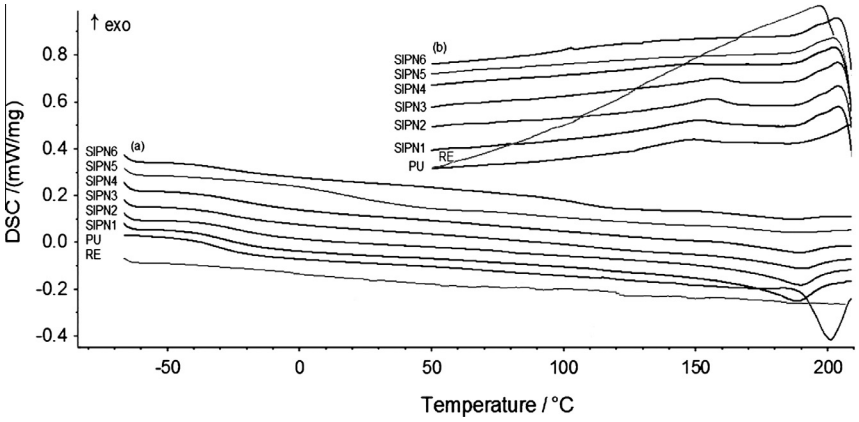

Fig. 1. DSC heating (a) and cooling (b) curves of the S-IPNs and of the initial polymers.

Table 1
Composition and T_g of the S-IPNs.

Sample	PU (%)	ER (%)	T_g (°C)
PU	100	0	−32.7
SIPN1	95	5	−29.5
SIPN2	90	10	−25.67
SIPN3	85	15	−23.46
SIPN4	80	20	−21.31
SIPN5	70	30	15.74
SIPN6	60	40	−32.39 105.46
ERN	0	100	120

imum cross-linking degree. S-IPN-6 presents two T_g values, thus indicating phase separation.

3.2. Miscibility studies

Fox equation [20] (Eq. (1)), was used in order to carry out the variation of T_gs of the blends vs. composition (% ERN).

$$\frac{1}{T_g} = \frac{w_1}{T_{g,1}} + \frac{w_2}{T_{g,2}} \tag{1}$$

where w_1 and w_2 are the weight fractions, and $T_{g,1}$ and $T_{g,2}$ are T_gs of the two starting polymers.

The results obtained using both the experimental data and the Fox equation are shown in Fig. 2. The positive deviation between the experimental and theoretical values, as can be observed in Fig. 2, is evidence of the presence of some specific interactions which lead to good miscibility between the two polymers in the studied S-IPNs [21,22].

An appreciation of the strength of the interaction between the two pure polymers in the S-IPNs was performed using the Gordon–Taylor equation [23], shown in the following equation:

$$T_{g,1} - T_{g,2} = \frac{k_{GT} w_1 (T_g - T_{g,2})}{w_2} \tag{2}$$

where k_{GT} is a constant which indicates the strength of the interactions in the studied S-IPNs and which has to be evaluated from experimental data.

Fig. 3 indicates the plot $T_g - T_{g,1}$ vs. $w_2(T_{g,2} - T_g)/w_1$. It can be observed that the plot in Fig. 3 is a typical characteristic S-shaped curve showing negative and positive deviations from the Gordon–Taylor equation. Using the Gordon–Taylor equation a straight line was obtained, with a slope value of k_{GT} = 1.9392. If the value were to be close to unity, it would suggest that the interactions between the two studied polymers would not be very strong [24]. However, in this case, a value close to 2 suggests the opposite.

Miscibility studies may be correlated with thermal behavior in inert atmosphere. Authors reported in a previous paper that samples containing up to a maximum of 10% epoxy resin started

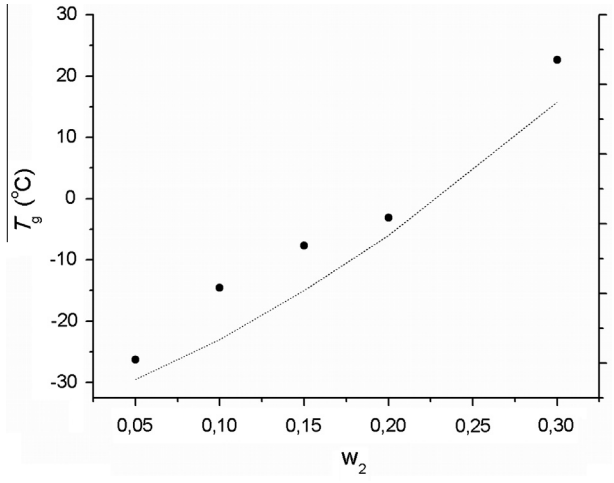

Fig. 2. Plot of T_g against composition for S-IPNs: (●) experimental T_g vales; (--) theoretical plot based on the Fox equation.

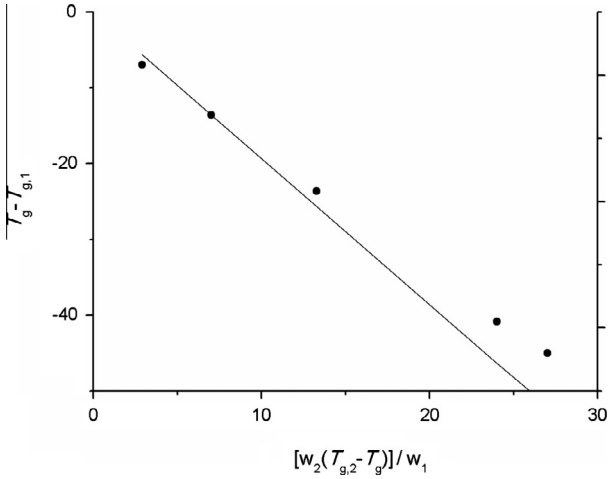

Fig. 3. Plot of $T_g - T_{g,1}$ vs. $w_2(T_{g,2} - T_g)/w_1$ (Gordon–Taylor equation) for the S-IPNs: (●) experimental T_g values; (—) Gordon–Taylor equation.

decomposing at temperatures between those of pure components, suggesting the existence of weak interactions between the pure comprising contents. Samples with a higher than 10% content of epoxy resin decomposed at temperatures below that of the polyurethane. The higher the ERN content, the lower the thermal stability [14]. Such behavior could be attributed to an intensification of the specific interactions between pure components which lead to a slight decrease in thermal stability [25]. The existence of these specific interactions were determined by dynamic mechanical analysis and reported in a previous paper [26]. Concentrations of cross-linked resin up to 10% in the S-IPN structure enhance the macromolecules mobility in polyurethane as a result of lessening of the hydrogen bonds between hard segments and soft/hard segments domains. When the epoxy resin content exceeds 10% it controls the material rigidity and at 40% ERN content in S-IPNs the movements of soft segments are totally hindered [26].

3.3. Absolute heat capacities and cross-linking densities determination

According to the literature, one of the proposed methods for determining cross-linking density values requires absolute heat capacities values determination [27]:

$$\rho'_c = \frac{C_p^i - C_p^0}{C_p^0} = \frac{\Delta C_p^i}{C_p^0} \tag{3}$$

where C_p^i and C_p^0 are the heat capacities of the network at a given cross-linking density, $(\rho'_c)^i$, and that of the pure PU, respectively. In order to determine the heat capacities, three measurements were carried out for each sample: (1) measurements with empty crucibles; (2) measurements with a reference material (pure sapphire) with a known specific heat capacity [28]; (3) measurements of the specific heats of S-IPNs (Fig. 3). The relationship between the heat capacity of the sample, C_p (sample), consisting in sample pan support + sample pan + sample, of the reference material, C_p (reference), consisting in reference material support + reference material pan + reference material and the heating rate (β) can be expressed as the following equation [29]:

$$C_p(\text{sample}) - -C_p(\text{reference}) = \frac{T(\text{sample}) - T(\text{reference})}{\beta R} \tag{4}$$

where T(sample) is the temperature of the sample; T(reference) is the temperature of the pure sapphire; R is the instrument constant (resistance between sample, reference material and furnace) and T(sample) − T(reference) is the DSC displacement, which is proportional to the difference between C_p (sample) and C_p (reference). If the DSC displacement is D and the proportionality constant is k, Eq. (4) becomes Eq. (5):

$$C_p(\text{sample}) - C_p(\text{reference}) = kD \tag{5}$$

The heat capacities of the sample support and the reference material support can be noted C_p^h(sample) and C_p^h(reference), the specific heat capacities of the reference material and sample can be represented by c_r and c_s, and the mass of the reference material and of the sample, m_r and m_s, respectively, leading to the obtaining of the following equations:

$$C_p^h(\text{sample}) - C_p^h(\text{reference}) = kD_1 \tag{6}$$

$$(C_p^h(\text{sample}) + m_r c_r) - C_p^h(\text{reference}) = kD_2 \tag{7}$$

$$(C_p^h(\text{sample}) + m_s c_s) - C_p^h(\text{reference}) = kD_3 \tag{8}$$

where D_1, D_2, D_3 are the effective thermal displacements of the DSC related to the blank, the reference and the sample.

From Eqs. (6)–(8), Eq. (9) is obtained:

$$\frac{m_s c_s}{m_r c_r} = \frac{D_3 - D_1}{D_2 - D_1} \tag{9}$$

Since the specific heat capacity of the reference material is known, the heat capacity of the samples can be calculated using the following equation:

$$C_p(\text{sample}) = \frac{m_r c_r}{m_s}\frac{D_3 - D_1}{D_2 - D_1} \tag{10}$$

D_1, D_2, D_3 are continuous functions related to the temperature, consequently the specific heat capacities can be determined continuously [30]. Heat capacities were calculated for the approximate temperature corresponding to the end of the T_g process for each studied sample. Heat capacity values and cross-linking density values are given in Table 2. It can be observed that T_g and cross-linking density values increase with the heat capacity values decrease, as expected. The heat capacity is an energetic characteristic of the chain segments movement. Upon increasing values of the cross-linking degree, reduction of free volume between chain segments sterically hinders their movement, thus lowering the heat capacity values [27].

3.4. Morphological studies

The microstructure of both ERN and PU is very important because it has profound effects on the morphology, thermal and mechanical properties [31]. Binder and Frisch have suggested that apparently miscible interpenetrating networks (IPNs) could form from polymers with immiscible linear chains. According to Frisch the condition of miscibility of IPNs does not consist solely on the existence of a single T_g. The absence of discernible phase domains, demonstrated by microscopic techniques, is also a mandatory criterion [32]. IPNs and S-IPNs often exhibit microphase separation inside the miscibility gap, as opposed to linear polymer blends, which undergo macrophase separation [8]. This aspect leads to the formation of a macroscopic dispersed phase with divided phase domains. These phase domains, each rich in a particular polymer species, interpenetrate each other in a highly cross-linked structure and often undetectable by SEM in a highly miscible S-IPN system [33].

Fig. 4 displays the OM micrographs of the S-IPNs. The formation of the S-IPNs can be clearly observed for S-IPN-1 (Fig. 4a), S-IPN-2 (Fig. 4b), S-IPN-3 (Fig. 4c) and S-IPN-4 (Fig. 4d). When the cross-linking density of the ERN network increases (20%, 30% and 40%), the resulting S-IPNs show more compact structures (Fig. 4d–f). Phase separation is clearly evidenced for S-IPN-6 (Fig. 4f). This aspect is in good agreement with the DSC results.

Fig. 5 shows the SEM images of the S-IPNs and the initial polymers. The ERN micrograph (Fig. 5b) depicts a sea-island morphology. The same aspect can be noticed for the S-IPN-5 (Fig. 5g) and S-IPN-6 (Fig. 5h) structures with the apparition of ERN islands having sizes in the range 1.03–7.80 μm for S-IPN-5 and 4.05–8.86 μm for S-IPN-6. Although this aspect demonstrates the occurring of phase separation, the difference in micrographs from Fig. 5g and h is just slightly discernible and not in total correlation with the DSC data

Table 2
Heat capacities and related cross-linking data.

Sample	Heat capacity, C_p (J g^{-1} °C^{-1})	ρ'_c (mol cm^{-3})
PU	1.485	–
S-IPN-1	1.466	0.0128
S-IPN-2	1.417	0.0458
S-IPN-3	1.335	0.101
S-IPN-4	1.290	0.131
S-IPN-5	1.172	0.210

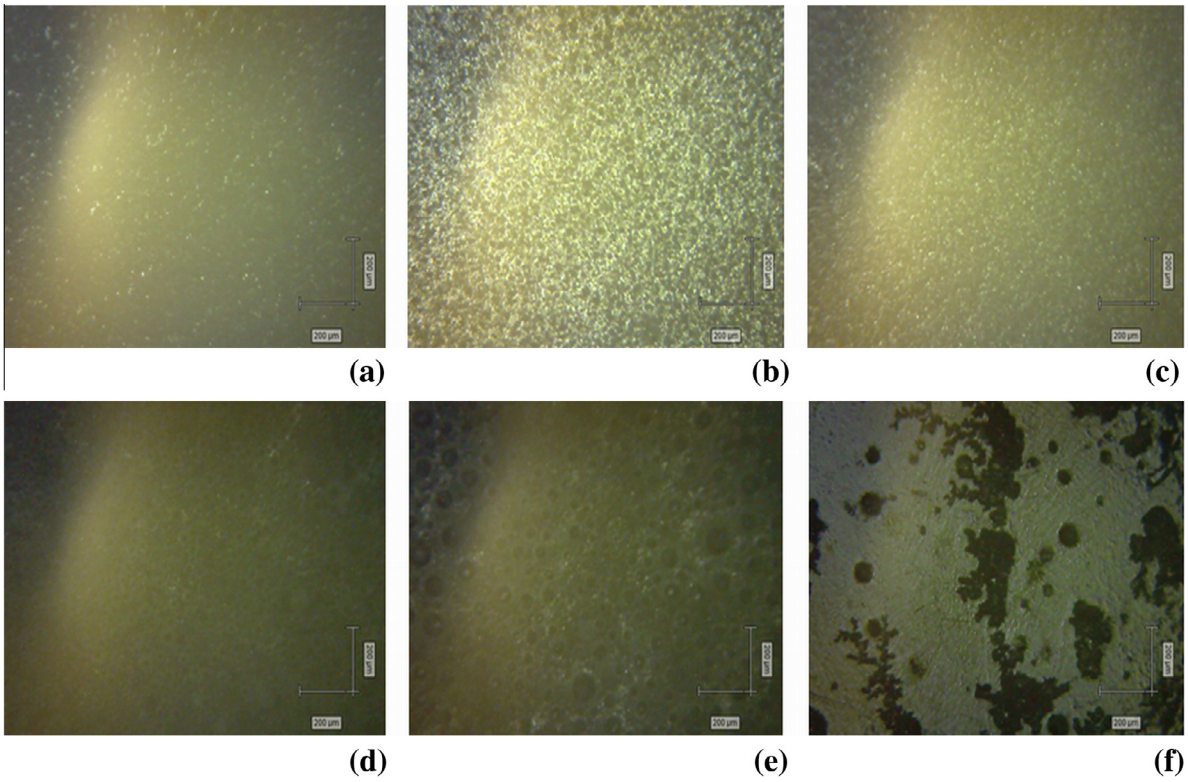

Fig. 4. OM micrographs of S-IPN-1 (a), S-IPN-2 (b), S-IPN-3 (c), S-IPN-4 (d), S-IPN-5 (e) and S-IPN-6 (f).

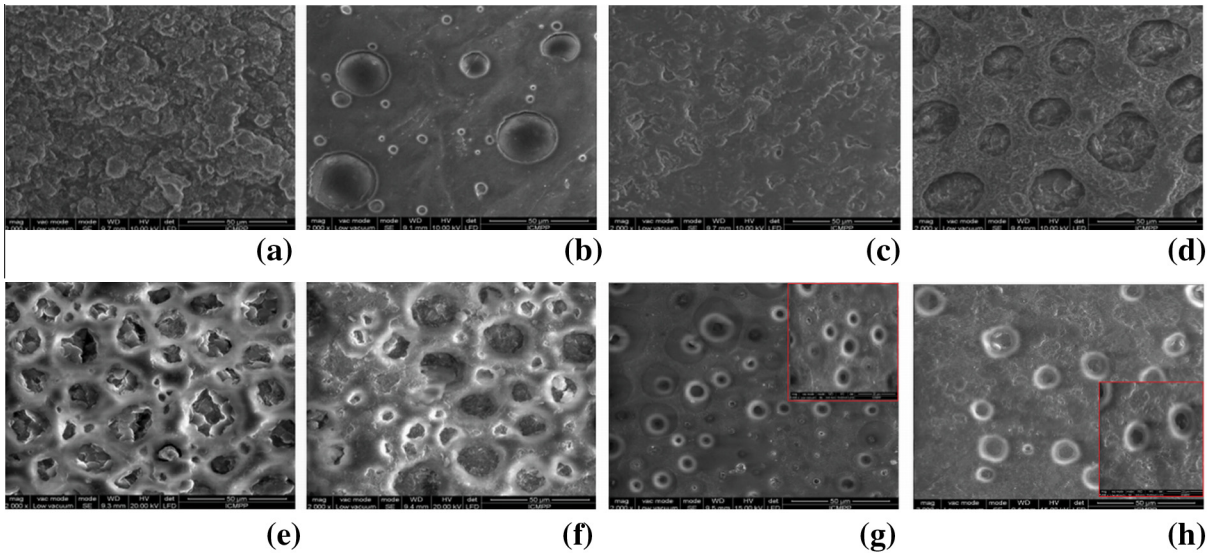

Fig. 5. SEM micrographs of PU (a), ERN (b), S-IPN-1 (c), S-IPN-2 (d), S-IPN-3 (e), S-IPN-4 (f), S-IPN-5 (g) and S-IPN-6 (h).

which showed phase separation occurring for sample S-IPN-6. This aspect was elucidated by recording the OM micrographs discussed above (Fig. 4).

4. Conclusions

Obtaining of S-IPNs offers attractive opportunities for developing new multicomponent materials with enhanced preordained properties. The S-IPNs based on an aromatic PU and increasing ERN content (5%, 10%, 15%, 20%, 30%, 40%) showed a good miscibility, up to an ERN content of 30%, which was established by the presence of a single T_g. DSC measurements and microscopy studied (OM, SEM) indicated phase separation for an ERN content of 40% in the S-IPN structures. Miscibility studies were conducted by applying the Fox and Gordon–Taylor equations and the results were in good correlation with the data obtained from the characterization methods. Cross-linking densities were determined for the S-IPNs and their values increase with heat capacity values decrease, as expected.

Acknowledgements

This work was supported by a grant of the Romanian National Authority for Scientific Research, CNCS – UEFISCDI, Project Number PN-II-ID-PCE-2011-3-0187.

Authors are grateful to Dr. Constantin Ciobanu, Dr. Laura Ursu and Ph.D. student Florica Doroftei of the "Petru Poni" Institute of Macromolecular Chemistry, Iasi, Romania for the polyurethane synthesis and OM and SEM micrographs.

References

[1] Lee H, Neville K. Handbook of epoxy resins. New York: McGraw-Hill Inc.; 1967.
[2] Ellis B. Chemistry and technology of epoxy resins. New York: Chapman& Hall; 1993.
[3] Poter HG. Epoxide resins. New York: Springer Verlag; 1970.
[4] Li ZH, Huang YP, Ren DY, Zheng ZQ. Structural characterization and properties of polyurethane modified TDE-85/MeTPHPA epoxy resin with interpenetrating polymer networks. J Cent S Univ Technol 2008;15:305–8.
[5] Rivaton A, Moreau L, Gardette JL. Photo-oxidation of phenoxy resins at long and short wavelengths-I. Identification of the photoproduct. Polym Degrad Stab 1997;58:321–32.
[6] Delor-Jestin F, Drouin D, Cheval PY, Lacoste J. Thermal and photochemical ageing of epoxy-resin-Influence of curing agents. Polym Degrad Stab 2006;91:1247–55.
[7] Paul DR. Polymer blends, phase behaviour and property relationship. In: Paul DR, Sperling LH, editors. Multicomponent polymer materials. Advances in Chemistry Series 211. Washington (DC): American Chemical Society; 1986. p. 3–20.
[8] Klempner D, Sperling LH, Utraki LA, Interpenetrating polymer networks. Advances in Chemistry Series 239. Washington (DC): American Chemical Society; 1994.
[9] Lipatov YS. Polymer blends and interpenetrating polymer networks at the interface with solids. Prog Polym Sci 2002;27:1721–801.
[10] Rosu L, Cascaval CN, Ciobanu C, Rosu D, Ion ED, Morosanu C, et al. Effect of UV radiation on the semi-interpenetrating polymer networks based on polyurethane and epoxy maleate of bisphenol A. J Photochem Photobiol A Chem 2005;169:177–85.
[11] Cascaval CN, Rosu D, Rosu L, Ciobanu C. Thermal degradation of semiinterpenetrating polymer networks based on polyurethane and epoxy maleate of bisphenol A. Polym Test 2003;22:45–9.
[12] Rosu D, Ciobanu C, Cascaval CN. Polyhydroxyacrylate-polyurethane semiinterpenetrating polymer network. Eur Polym J 2001;37:587–95.
[13] Rosu D, Rosu L, Mustata F, Varganici CD. Effect of UV radiation on some semi-interpenetrating polymer networks based on polyurethane and epoxy resin. Polym Degrad Stab 2012;97:1261–9.
[14] Rosu D, Rosu L, Varganici CD. The thermal stability of some semi-interpenetrated polymer networks based on epoxy resin and aromatic polyurethane. J Anal Appl Pyrol 2013;100:103–10.
[15] Jia Q, Zheng M, Chen H, Shen R. Morphologies and properties of polyurethane/epoxy resin interpenetrating network nanocomposites modified with organoclay. Mater Lett 2006;60:1306–9.
[16] Harrison IR, Runt JJ. Incompatible blends: thermal effects in a model system. J Polym Sci: Polym Phys 1980;18:2257–61.
[17] Aubin M, Bédard J, Marrissette M-F, Prud'homme RE. Miscible blends prepared from two crystalline polymers. J Polym Sci: Polym Phys 1983;21:223–40.
[18] Srikant SK, Arjumand AK, Mrityunjaya IA, Mahadevappa YK. Synthesis and characterization of hybrid membranes using poly(vinyl alcohol) and tetraethylorthosilicate for the pervaporation separation of water–isopropanol mixtures. J Appl Polym Sci 2004;94:1304–15.
[19] Hsu YG, Lin FJ. Organic–inorganic composite materials from acrylonitrile–butadienestyrene copolymers and silica through an in situ sol–gel process. J Appl Polym Sci 2000;75:275–83.
[20] Fox TGBull. Influence of diluent and of copolymer composition on the glass temperature of a polymer system. Am Phys Soc 1956;1:123.
[21] Singh VB, Walsh DJ. The miscibility of polyethersulfone with phenoxy resin. J Macromol Sci-Phys, Part B 1986;25:65–87.
[22] Lu S, Pearce EM, Kwei TK. Synthesis and characterization of (4-vinylphenyl)dimethylsilanol polymer and copolymers. Macromolecules 1993;26:3514–8.
[23] Gordon M, Taylor J. Ideal copolymers and the second-order transitions of synthetic rubbers. I. Non-crystalline copolymers. J Appl Chem 1952;2:493–500.
[24] Ciobanu C, Rosu D, Cascaval CN, Rosu L. Polyurethane-epoxy maleate of bisphenol A blends. J Macromol Sci-Pure Appl Chem, Part A 2001;38:991–1005.
[25] Mohamed A, Gordon SH, Biresaw G. Polycaprolactone/polystyrene bioblends characterized by thermogravimetry, modulated differential scanning calorimetry and infrared photoacoustic spectroscopy. Polym Degrad Stab 2007;92:1177–85.
[26] Cristea M, Ibanescu S, Cascaval CN, Rosu D. Dynamic mechanic analysis of polyurethaneepoxy interpenetrating polymer networks. High Perform Polym 2009;21:608–21.
[27] Varganici CD, Ursache O, Gaina C, Gaina V, Simionescu BC. Studies on new hybrid materials prepared by both Diels–Alder and Michael addition reactions. J Therm Anal Calorim 2013;111:1561–70.
[28] Furukawa GT, Douglas TB, McCloskey RE, Ginnings DC. Thermal properties of aluminum oxide from 0 K to 1200 K. J Res Nat Bur Stand 1956;57:67–82.
[29] Santos JCO, Santos MGO, Dantas JP, Conceição MM, Athaide-Filho PF, Souza AG. Comparative study of specific heat capacities of some vegetable oils obtained by DSC and microwave oven. J Therm Anal Calorim 2005;7:283–7.
[30] Santos JCO, Santos IMG, Conceição MM, Porto SL, Trindade MFS, Souza AG, et al. Thermoanalytical, kinetic and rheological parameters of commercial edible vegetable oils. J Therm Anal Cal 2004;75:419.
[31] Lim BY, Kim SC. Morphology of cross-linked poly(butyl methacrylateco-methyl methacrylate) porous membranes. J Membr Sci 2002;209:293–307.
[32] Frisch HL. Factors affecting the miscibility of simultaneous IPNs and pseudo-IPNs. Progr Org Coat 1996;27:67–72.
[33] Wu X, He G, Gu S, Hu Z, Yao P. Novel interpenetrating polymer network sulfonated poly (phthalazinone ether sulfone ketone)/polyacrylic acid proton exchange membranes for fuel cell. J Membr Sci 2007;295:80–7.